Multiferroic Phase Transition near Room Temperature in $BiFeO_3$ Films

I. C. Infante,[1,2] J. Juraszek,[3] S. Fusil,[1] B. Dupé,[2,4] P. Gemeiner,[2] O. Diéguez,[5] F. Pailloux,[6,7] S. Jouen,[3] E. Jacquet,[1] G. Geneste,[2,4] J. Pacaud,[6] J. Íñiguez,[5] L. Bellaiche,[8] A. Barthélémy,[1] B. Dkhil,[2] and M. Bibes[1,*]

[1]*Unité Mixte de Physique CNRS/Thales, Campus de l'Ecole Polytechnique, 1 avenue Fresnel, 91767 Palaiseau, France and Université Paris-Sud, 91405, Orsay, France*

[2]*Laboratoire Structures, Propriétés et Modélisation des Solides, UMR 8580 CNRS-Ecole Centrale Paris, Grande Voie des Vignes, 92295 Châtenay-Malabry Cedex, France*

[3]*Groupe de Physique des Matériaux, UMR6634 CNRS-Université de Rouen, F-76801 St. Etienne du Rouvray, France*

[4]*CEA-DAM DIF, F-91297 Arpajon, France*

[5]*Institut de Ciència de Materials de Barcelona (ICMAB-CSIC), Campus UAB, E-08193 Bellaterra, Spain*

[6]*Institut Pprime, UPR 3346 CNRS-Université de Poitiers-ENSMA, SP2MI, 86962 Futuroscope-Chasseneuil Cedex, France*

[7]*Canadian Center for Electron Microscopy, Brockhouse Institute for Materials Research, McMaster University, 1280 Main Street West, Hamilton, Ontario L8S4M1, Canada*

[8]*Physics Department, University of Arkansas, Fayetteville, Arkansas 72701, USA*

(Received 25 May 2011; published 30 November 2011)

In multiferroic $BiFeO_3$ thin films grown on highly mismatched $LaAlO_3$ substrates, we reveal the coexistence of two differently distorted polymorphs that leads to striking features in the temperature dependence of the structural and multiferroic properties. Notably, the highly distorted phase quasiconcomitantly presents an abrupt structural change, transforms from a standard to a nonconventional ferroelectric, and transitions from antiferromagnetic to paramagnetic at 360 ± 20 K. These coupled ferroic transitions just above room temperature hold promises of giant piezoelectric, magnetoelectric, and piezomagnetic responses, with potential in many applications fields.

DOI: 10.1103/PhysRevLett.107.237601 PACS numbers: 77.55.Nv, 75.30.Kz

Multiferroics that display simultaneously magnetic, polar, and elastic order parameters are gaining much attention due to their fascinating fundamental physics [1] as well as their considerable application potential [2,3]. Among them, $BiFeO_3$ (BFO) is intensively studied because both ferroelectric and magnetic orders coexist at room temperature (RT) [4]. Below the Curie temperature $T_C \approx 1100$ K, BFO is described by the rhombohedral $R3c$ space group, which allows antiphase octahedral tilting and ionic displacements from the centrosymmetric positions about and along the same $\langle 111 \rangle$ cubiclike direction. Bulk BFO is also a G-type antiferromagnet (AFM) with a cycloidal spin modulation below the Néel temperature $T_N = 640$ K.

The coexistence of ferroic orders with several lattice instabilities makes BFO an interesting playground to investigate strain engineering [5–7]. In particular, a novel "T-like" phase with giant tetragonality [8–10] and enhanced properties [11] was revealed for misfit strains of $\sim -5\%$. Also, and in contrast with the situation in more "classical" ferroelectrics like $BaTiO_3$ [12] it was found that compressive strain depresses T_C while leaving T_N almost unchanged, as a consequence of the subtle interplay between polarization and oxygen octahedral tilts [5]. For compressive strain values lower than -2.5% T_C and T_N should meet [5], extending the interest of BFO films as the magnetoelectric response should then be enhanced [13,14].

Here we show that AFM and ferroelectric phase transitions occur quasiconcomitantly in BFO films deposited onto (001)-oriented $LaAlO_3$ (misfit strain of -4.8%). Remarkably, this multiferroic phase transition takes place just above RT, in a range of interest for applications. Combining temperature-dependent x-ray diffraction (XRD), piezoresponse force microscopy (PFM) and Mössbauer (MS) spectroscopy techniques, we evidence that both transitions occur in the temperature domain of 340–380 K. These findings are supported by theoretical calculations based on first principles.

The films were grown by pulsed laser deposition in conditions reported elsewhere [9,15]. The 70 nm-thick sample used for MS was grown using a $\sim 100\%$ ^{57}Fe enriched target. For PFM measurements, an 11 nm-thick fully strained $La_{2/3}Sr_{1/3}MnO_3$ (LSMO) bottom electrode was used. Symmetric x-ray diffraction (XRD) $2\theta - \omega$ scans indicated a majority phase with a large c-axis parameter of 4.67 Å (corresponding to the T-like phase; in-depth analysis of electron microscopy results not presented here suggests a crystallization in a Cm space group), while asymmetric scans indicated the presence of an additional R-like phase. This phase coexistence is confirmed by high resolution transmission electron microscopy (HRSTEM). Figure 1(a) displays a bright field image and Fig. 1(b) the corresponding diffraction pattern. Digital dark field images were calculated from the Fourier transform (FT) of the HRSTEM image by selecting a spot of a given phase and performing an inverse FT. In this FT, three families of spots can be identified along the growth direction: the LAO substrate [Fig. 1(c)], T-like BFO with a large c/a ratio [Fig. 1(d)] and R-like BFO with the c axis tilted about 3°

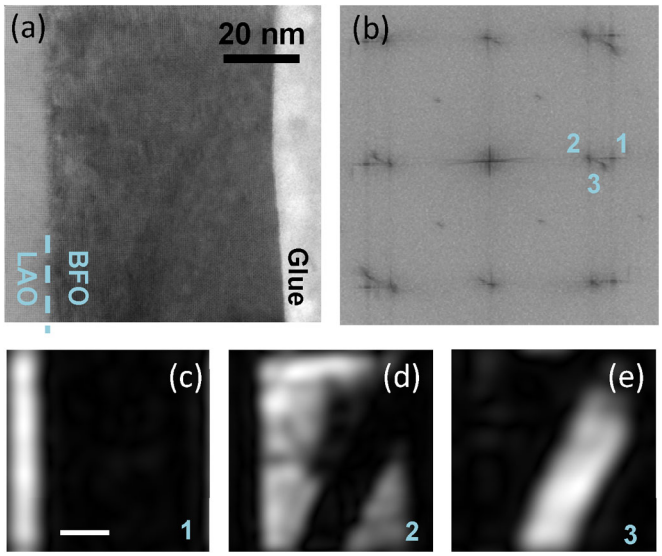

FIG. 1 (color online). (a) Bright field image of a BFO film, (b) FT of (a) showing spots coming from the different phases (labeled 1, 2, and 3), (c)–(e) digital dark field images of the considered spots. The white scale bar in (c) corresponds to 20 nm.

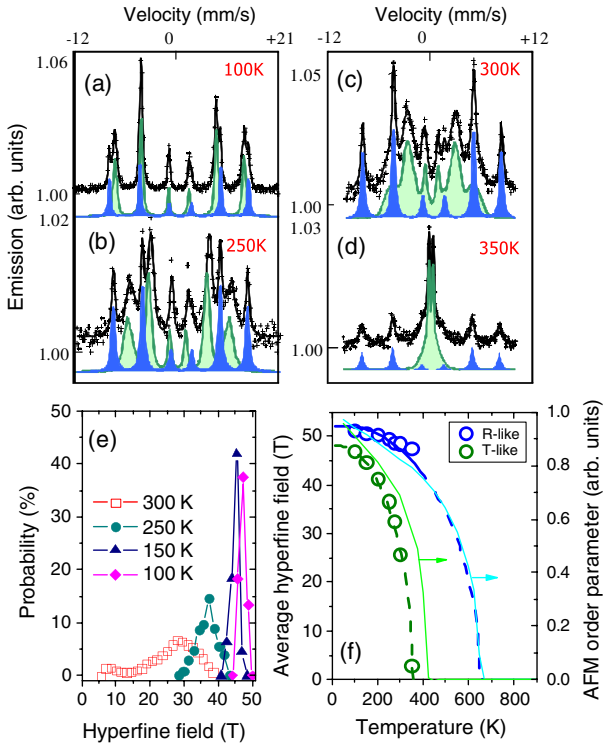

FIG. 2 (color online). ^{57}Fe Mössbauer spectra of the BFO// LAO film at 100 K (a), 250 K (b), 300 K (c), and 350 K (d) fitted by two magnetic subspectra (blue: R-like and green: T-like). Hyperfine field distributions of the T-like component at different temperatures (e) and temperature dependence of the average hyperfine fields (f). Dashed lines are Brillouin functions for Fe^{3+} ($S = 5/2$) fitted to the data; solid lines correspond to model Hamiltonian simulations.

from the growth direction [Fig. 1(e)]. The R-like diffraction can then be attributed to the large slanted grain and the main T-like phase is visible in the rest of the image. Using the geometric phase analysis method, the average out-of-plane and in-plane lattice parameters for the T-like and R-like phases are $c = 4.66$ Å and $a = 3.79$ Å, and $c = 4.10$ Å and $a = 3.91$ Å, respectively. The R phase thus experiences a -1.3% compressive strain, as in BFO films grown on $SrTiO_3$ [5].

^{57}Fe Mössbauer spectra were measured using the conversion electron technique (CEMS) which allows the characterization of thin films [16]. The spectra were collected under normal incidence using a gas-flow proportional counter mounted inside a closed cycle Janis cryostat, and a ~50 mCi ^{57}Co radioactive source in a Rh matrix in constant acceleration mode. The isomer shift is given with respect to α-Fe at 300 K. Figures 2(a)–2(d) displays the spectra at different temperatures. The data unambiguously show the contribution of two AFM components associated with two different sets of magnetically split sextets between 100 and 300 K. Isomer shifts values ($\delta = 0.31$–0.37 mm/s) for both components are characteristic of Fe^{3+} ions in octahedral coordination. At 100 K, the spectrum exhibits a sharp sextet with a magnetic hyperfine field $B_{hf} = 51$ T and a slightly broader one fitted with a narrow magnetic hyperfine field distribution $P(B_{hf})$ centered at $B_{hf} = 47$ T. The sharp sextet has a B_{hf} close to that of bulk BFO and is identified to the R-like phase, whereas the less magnetic component is identified to the T-like phase. Both subspectra are very similar to the spectrum recorded for BFO grown on $GdScO_3$ (GSO) [5] indicating that low temperature antiferromagnetism is G type. It should be noted that the line intensity ratio R_{23} of the second and third lines of each Zeeman sextet is close to 4.0, evidencing the in-plane orientation of the Fe^{3+} magnetic moments for both phases.

The spectral area ratio between both magnetic phases represents roughly 2/3 (T-like) and 1/3 (R-like) of the sample volume at all temperatures, meaning that one phase does not transform into the other. In fact, the coexistence of both phases is not an unexpected feature considering their energy diagrams as a function of misfit strain [17,18]. We argue that the minority phase allows the stabilization of the giant tetragonality majority phase. Indeed, the T phase is associated with a misfit strain of -4.8%, whereas the addition of 1/3 of R phase with a misfit strain of -1.3% would decrease the global misfit strain felt by the BFO film to $\sim -3.6\%$.

Upon increasing temperature up to 300 K, the overall splitting of the outer emission lines, that measures the average effective B_{hf} at the nucleus, drastically decreases for the T-like component, revealing the approach of a magnetic phase transition [Figs. 2(b)–2(d)]. The corresponding $P(B_{hf})$ distribution becomes broader and its maximum is progressively shifted to lower fields

[Fig. 2(e)]. The temperature dependence of the average B_{hf} for both the T-like and R-like phases, and their fits using a mean field model are shown in Fig. 2(f). For the T phase they indicate a $T_N \approx 360$ K far from the bulk value of 640 K. The same analysis for the R-like phase yields a T_N of ≈ 640 K as expected from the calculated phase diagram based on a monoclinic Cc ground state [5].

The proximity of the T_N for the T phase with RT is also confirmed by our simulations. It has been shown [19] that the magnetic interactions in BFO supertetragonal phases are characterized by a strong splitting of the in-plane (J_{ab}) and out-of-plane (J_c) couplings between nearest-neighboring Fe spins. Further, the basic magnetic properties can be captured in a simple Heisenberg Hamiltonian ($E = E_0 + \frac{1}{2} J_{ij} S_i S_j$, with $|S_i| = 1$ and the sum being limited to first-nearest neighbors) with $J_{ab} \approx 40$ meV and $J_c \approx 4$ meV. We solved such a model using standard Monte Carlo techniques and obtained the temperature dependence of the AFM order parameter shown with solid lines in Fig. 2(f); the computed T_N is about 425 K, in reasonable agreement with our Mössbauer data for the T-like phases. (We checked that the computed T_N remains essentially unchanged upon ± 2 meV variations of the coupling constants.) In Fig. 2(f) we also show the simulation results for the analogous Heisenberg Hamiltonian corresponding to BFO's bulklike phase (defined by $J_{ab} = J_c = 38$ meV); in this case we obtained $T_N \simeq 650$ K, in good agreement with the experimental value of 640 K for the R-like phase. Our theory thus confirms that the majority T-like and minority R-like phases in our films present a markedly different temperature dependence of their magnetic properties, as well as distinct magnetic critical temperatures. From this analysis, we conclude that the films consist of a mixture of a 1.3% strained R-like phase, whose physical properties are described in Ref. [5], and a poorly known T-like phase that we discuss further in the following.

We characterized the structural properties as a function of temperature using XRD [5,20]. Figure 3(a) displays the thermal variation of the c-axis parameters of the T-like phase and the substrate. The c-axis parameter increases rapidly as temperature rises before reaching a plateau above ~340 K (heating) or ~370 K (cooling). The plateau spreads over 150 K before the c-axis parameter starts to decrease continuously upon increasing temperature. While another change of behavior is visible at ~700 K and might be evidence for a structural modification, the abrupt change at 340–370 K appears as a signature of a reversible structural phase transition with hysteresis. As the elastic change is rather strong, it cannot be directly due to the AFM to paramagnetic phase transition that we evidenced using MS [5,20,21]. More likely, this transition is related to a ferroelectric phase transition. More insight on this point is gained from the temperature dependence of the (103) reflection. As visible in Fig. 3(b), its normalized intensity

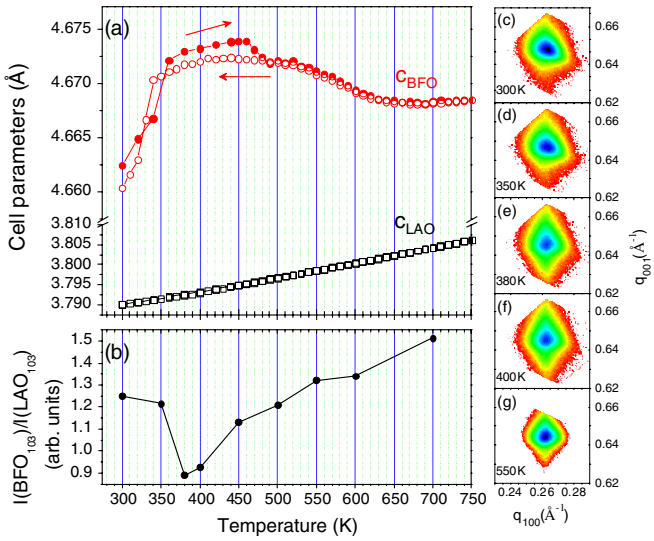

FIG. 3 (color online). (a) Temperature dependence of the c axis parameters of the T-like phase of the BFO film and of the LAO substrate. (b) Temperature dependence of the relative intensity of the (103) reflections from the T-like BFO phase and the LAO. (c)–(g) Reciprocal space maps of the (103) reflection of the T-like BFO phase for different temperatures.

shows an obvious change of behavior at ~380 K. Its shape also changes from asymmetric [Fig. 3(c)], in agreement with a monocliniclike phase [10,22], to symmetric above 370 K [Figs. 3(e)–3(g)], which strongly suggests that beyond the transition the phase is more tetragonal-like. Complementary Raman spectroscopy measurements (not shown) also indicate a phase transition occurring at ~380 K.

To explore the ferroelectric nature of this phase transition we characterized the ferroelectric properties using PFM. Piezoelectric loops were recorded while heating the samples *in situ* up to 498 K. At RT, loops can consistently be measured irrespective of the tip position on the sample, as expected for a standard ferroelectric; see Figs. 4(a) and 4(g) (inset). However, at high temperatures, the response shows a strong variability with tip position; i.e., either loops with low coercive field values [Figs. 4(c)–4(f)] can be recorded or there is no response at all. This suggests that BFO//LAO exhibits a transition toward a phase with qualitatively different ferroelectric or ferroelectriclike response whose precise nature remains to be determined. As inferred from the dependence of the coercive voltage on temperature shown in Fig. 4(g), this transition occurs in the same temperature range as the detected magnetic and structural phase transitions.

In summary, we have found that in BFO films deposited onto LAO substrate a majority T-like phase and a minority R-like one coexist. We argued that such phase coexistence allows this system to release the huge misfit strain imposed by the substrate. Remarkably, the T-like phase exhibits both structural, magnetic, and ferroelectric phase

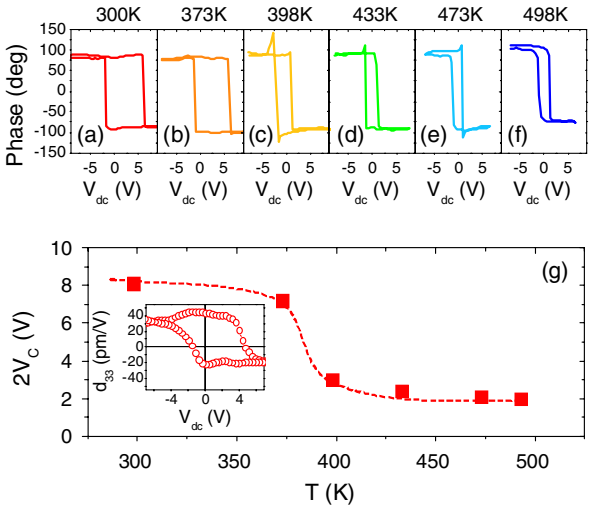

FIG. 4 (color online). (a)–(f) Selected piezoresponse phase vs voltage cycles measured in a BFO/LSMO//LAO film at different temperatures. (g) Temperature dependence of the coercive voltages extracted from the loops in (a)–(f). The dashed line is a guide to the eye. Inset: voltage dependence of the piezoelectric coefficient at room temperature.

transitions in a narrow temperature range around 360 K, as evidenced by XRD, Mössbauer spectroscopy, and PFM studies, respectively, and confirmed by theory. Our results thus demonstrate the possibility of engineering a multiferroic having its critical temperatures (and thus diverging dielectric and magnetic susceptibilities, piezoelectricy, magnetoelectricity, etc.) close to 300 K, which opens new paths for the use of BFO in applications.

We thank D. Colson, B. Warot-Fonrose, H. Béa, M. Couillard, and G. Botton. This work was supported by the French C-Nano Ile-de-France Magellan, PRES Universud Nano-Ox, ANR Pnano project "Méloïc," MICINN-Spain Grants No. MAT2010-18113, No. MAT2010-10093-E, No. CSD2007-00041, the ONR Grants No. N00014-04-1-0413, No. N00014-08-1-0915, and No. N00014-07-1-0825, NSF Grants No. DMR 0701558 and No. DMR-0080054, and the Department of Energy, Office of Basic Energy Sciences, under Contract No. ER-466120. Part of the microscopy work was carried out at the Canadian Centre for Electron Microscopy, a National Facility supported by NSERC and McMaster University.

Note added.—During the review process of this manuscript, two papers also reported a structural transition at about 370 K in T-like BFO [23,24].

*manuel.bibes@thalesgroup.com

[1] K. Wang, J.-M. Liu, and Z. Ren, Adv. Phys. **58**, 321 (2009).
[2] H. Béa, M. Gajek, M. Bibes, and A. Barthélémy, J. Phys. Condens. Matter **20**, 434221 (2008).
[3] M. Bibes, J. E. Villegas, and A. Barthélémy, Adv. Phys. **60**, 5 (2011).
[4] G. Catalan and J. F. Scott, Adv. Mater. **21**, 2463 (2009).
[5] I. C. Infante *et al.*, Phys. Rev. Lett. **105**, 057601 (2010).
[6] A. J. Hatt., N. A. Spaldin, and C. Ederer, Phys. Rev. B **81**, 054109 (2010).
[7] O. Diéguez, O. E. Gonzalez-Vazquez, J. C. Wojdel, and J. Iñiguez, Phys. Rev. B **83**, 0940105 (2011).
[8] D. Ricinschi, K.-Y. Yun, and M. A. Okuyama, J. Phys. Condens. Matter **18**, L97 (2006).
[9] H. Béa *et al.*, Phys. Rev. Lett. **102**, 217603 (2009).
[10] H. M. Christen, J. H. Nam, H. S. Kim, A. J. Hatt, and N. A. Spaldin, Phys. Rev. B **83**, 144107 (2011).
[11] R. J. Zeches *et al.*, Science **326**, 977 (2009).
[12] K. J. Choi *et al.*, Science **306**, 1005 (2004).
[13] J. C. Wojdel and J. Iñiguez, Phys. Rev. Lett. **105**, 037208 (2010).
[14] S. Prosandeev, I. A. Kornev, and L. Bellaiche, Phys. Rev. B **83**, 020102(R) (2011).
[15] H. Béa *et al.*, Appl. Phys. Lett. **87**, 072508 (2005).
[16] J. Juraszek, O. Zivotsky, H. Chiron, C. Vaudolon, and J. Teillet, Rev. Sci. Instrum. **80**, 043905 (2009); M. T. Sougrati, M. Jean, S. Jouen, C. Vaudolon, and B. Hannoyer, Hyperfine Interact. (in press).
[17] B. Dupé *et al.*, Phys. Rev. B **81**, 144128 (2010).
[18] Z. Chen *et al.*, arXiv:1104.4712v1.
[19] O. Diéguez and J. Iñiguez, Phys. Rev. Lett. **107**, 057601 (2011).
[20] H. Toupet, F. Le Marrec, C. Lichtensteiger, B. Dkhil, and M. Karkut, Phys. Rev. B **81**, 140101(R) (2010).
[21] R. Haumont *et al.*, Phys. Rev. B **78**, 134108 (2008).
[22] N. Noheda *et al.*, Phys. Rev. B **65**, 224101 (2002).
[23] W. Siemons, M. D. Biegalski, J. H. Nam, and H. M. Christen, Appl. Phys. Express **4**, 095801 (2011).
[24] J. Kreisel *et al.*, J. Phys. Condens. Matter **23**, 342202 (2011).